Synthesis, stability, and reactivity of mesoionic carbene iridium dihydride complexes

Marta Olivares[a] and Martin Albrecht*[a]

[a]Departement für Chemie und Biochemie, Universität Bern, Freiestrasse 3, CH-3012 Bern, Switzerland

* to whom correspondence should be addressed:

E-mail: martin.albrecht@dcb.unibe.ch

Phone: +41 31631 4644

Dedicated to Bob Morris in recognition of his pioneering work, in particular in hydrogen transfer chemistry

Abstract

Pyridyl-triazolylidene ligands with variable donor properties were used as tunable ligands at a dihydride iridium(III) center. The straightforward synthesis of this type of ligand allows for an easy incorporation of electron donating substituents in different positions of the pyridine ring or different functional groups such as esters, alkoxy or aliphatic chains on the C4-position of the triazole heterocycle. The stability of these hydride metal systems allowed these complexes to be used as models for studying the influence of the ligand modifications on hydride reactivity. Spectroscopic analysis provided unambiguous structural assignment of the dihydride system. Modulation of the electronic properties of the wingtip substituents did not appreciably alter the reactivity of the hydrides. Reactivity studies using acids with a wide range of pK_a values indicated a correlation between hydride reactivity and acidity and showed exclusive reactivity towards the less shielded hydride *trans* to the carbene carbon rather than the more shielded hydride *trans* to the pyridine ring, suggesting that the *trans* effect is more relevant in these reactions than the NMR spectroscopically deduced hydridic character.

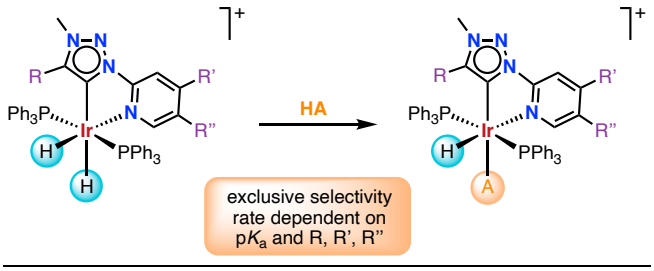

Introduction

Transition metal hydride complexes represent an important class of organometallic compounds because of their ability to function in a variety of catalytic and stoichiometric processes.[1] They are involved, for example, in energy conversion or hydrogen storage applications.[2,3] Metal hydride intermediates are also prevalent in reactions that involve C–H bond activation, such as transfer hydrogenation,[4,5,6,7] olefin isomerization,[8,9] and C–H functionalization.[10,11,12,13]

Understanding how changes in steric and electronic properties influence hydride transfer is of great importance in complex design in order to enhance stoichiometric and catalytic reactions involving metal hydrides. The term 'hydricity' is the most commonly used descriptor of hydride donor ability. The hydricity of a metal hydride therefore provides an experimentally measurable parameter that can help to predict the reactivity of a metal hydride. The two most common techniques for measuring the relative rates of hydride transfer to a reference substrate are NMR and UV-vis spectroscopy. Knowledge of cleaving metal hydride bonds enables the prediction of chemical reactivity, *e.g.* for bond-forming and bond-breaking events that occur in a catalytic reaction. Therefore, hydricity also connects fundamental bonding and reactivity studies with catalyst design principles and applications.[14]

Herein we introduce the facile reaction of triazolylidene precursor salts with a metal hydride precursor to obtain a new family of hydride iridium complexes. A major advantage of triazolylidene NHC ligands is their straightforward synthesis, which allows modifications to be introduced easily for fine-tuning the electronic and steric properties as a method to improve catalytic activity. We applied this concept through varying the substituents in different positions of the pyridyl ring and on the triazole heterocycle. All complexes are air-stable, which facilitates fundamental and reactivity studies that are considerably more difficult with more reactive hydride complexes or short-lived hydride intermediates. The stability of these iridium complexes is highly attractive for evaluating their behavior for the design of efficient catalysts and offers opportunities for materials science.[15]

Here, we have investigated the factors that favor hydride reactivity, such as electronic and steric variations of wingtip groups, *trans* influence/effects on the hydrides from the triazolylidene heterocycle or the pyridine ring, and the effect of acids with a wide range of pK_a values. Remarkably and counterintuitively, in these complexes the more shielded hydride is demonstrated to be less reactive.

Result and discussion

1. Synthesis and characterization of a series of dihydride iridium complexes with mesoionic carbene ligands. Metalation of the known[16,17] triazolium salts **1**–**3** was accomplished upon reaction with $IrH_5(PPh_3)_2$ in toluene at elevated temperature (Scheme 1), similar to related work

with imidazolium salts.[18] These conditions induced triazolium C–H bond activation *via* cyclometalation and afforded complexes **4**–**6** as pale yellow solids. All complexes were formed within 24 h. They were completely air- and moisture stable and were purified *via* standard column chromatography over silica in moderate yield and featured variable substituents on the triazolylidene unit (**4a**, **5**, **6**) and on the pyridyl site (**4a**, **4b**, **4c**).

Scheme 1. Synthesis of iridium complexes **4**–**6**.

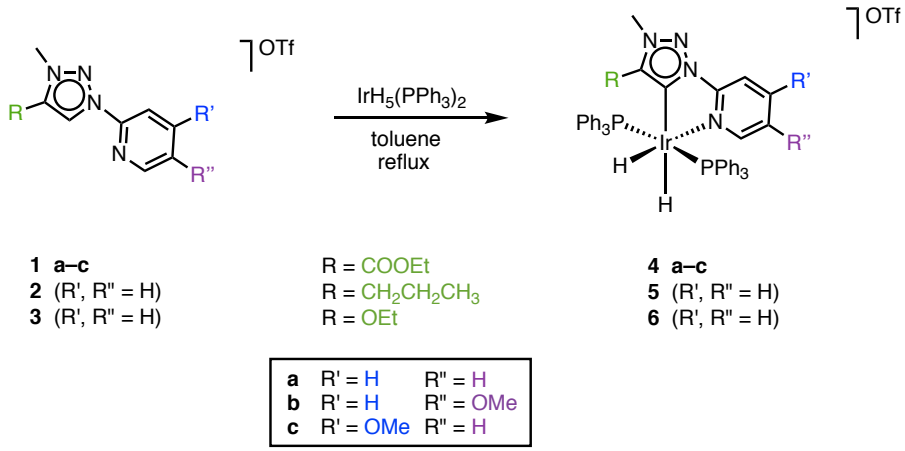

NMR characterization. All complexes were characterized by ^{1}H, ^{13}C and ^{31}P NMR spectroscopy, which are in good agreement with the proposed structures (Scheme 1). For all complexes, ^{1}H NMR spectroscopy confirms the coordination of two PPh_3 ligands as the phenyl resonances integrate for 30 H. These phosphine nuclei are equivalent since only one singlet is observed in the ^{31}P NMR spectrum, resonating around 19(±1) ppm. Moreover, all complexes show two inequivalent hydrides at high field resonances, both split into triplet of doublets by mutual coupling and coupling to two equivalent phosphorus nuclei. The J_{HH} of 5 Hz is typical of *cis*-positioned dihydrides,[19] and the J_{PH} of 17–20 Hz is characteristic of a *cis* $M(PR_3)H$ arrangement.[19] The metal-bound hydride resonances are separated by almost 10 ppm and appear around $\delta_H = -11$ and –20 ppm, reflecting the largely different influence of the triazolylidene and pyridine as *trans* ligands. So far, the assignment of this type of dihydride systems has been controversial in the literature.[18,20] Here, NOEs were detected between the hydride at –20 ppm and the CH_2 of the –OEt group ($\delta_H = 3.8$ ppm) of complex **6**, and additionally between the hydride at –11 ppm and the pyridyl C^6–H proton at around 8 ppm (Figure 1). These NOE experiments indicate therefore that the higher field hydride at –20 ppm is *cis* to the triazolylidene (denoted as H_{cis}) moiety and the lower field hydride (–11 ppm) is *cis* to the pyridyl ligand (denoted as H_{trans}). Similar NOE experiments were also run with complexes **4b** and **5**, and the results were in line with the assignments obtained for complex **6** (Fig. S1, S2). Notably, this experimental assignment

is counterintuitive when considering the higher *trans* influence of the carbene *vs* pyridine, and indicates that the NMR chemical shifts are not correctly reflecting hydricity.

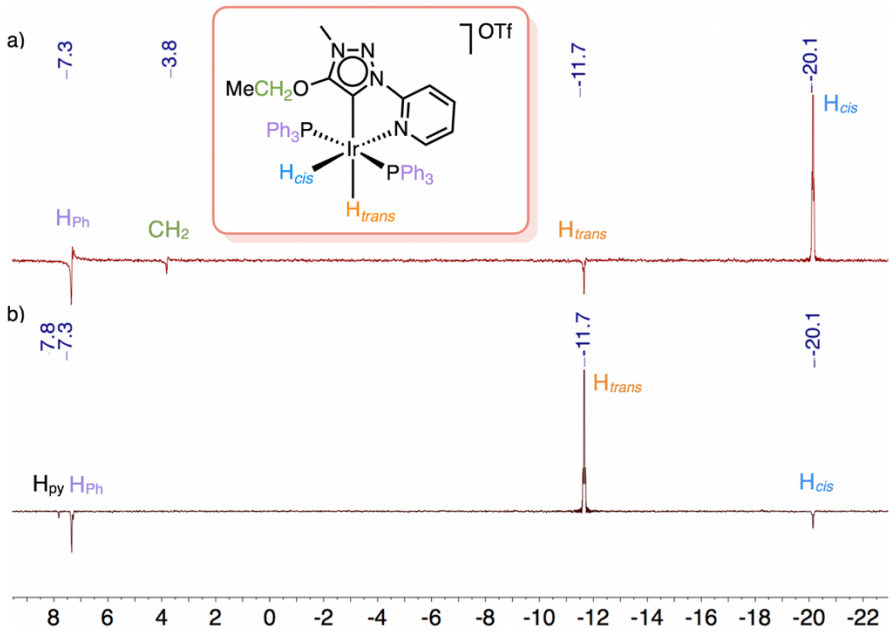

Figure 1. NOE experiment ($CDCl_3$, 400 MHz, 298 K) for assignment of hydride resonances using complex **6**. NOE correlations obtained from selective irradiation of a) the *cis* hydride resonance at –20 ppm and b) the *trans* hydride resonance at –11 ppm (*trans* and *cis* relative to the carbene ligand).

The influence of different electron donating/withdrawing substituent R on the triazolylidene donor site (R = –COOEt, –*n*Pr, or –OEt, Figure 2) is evident when comparing complexes **4a**, **5** and **6** containing the same pyridine moiety (Table 1). According to ^{13}C NMR analysis, the chemical shifts of the carbenic carbon, the N–CH_3 and the C_{trz}–R for complexes **4a** and **6** significantly differ, while the resonance frequencies of complex **5** always stay in between. Thus, the carbenic carbon significantly appears at lower field in complex **6** with an electron donating –OEt substituent compared to the presence of an electron-withdrawing –COOEt group in complex **4a** (δ_C = 175 and 146 ppm, respectively). A similar chemical shift divergence is also observed for the N–CH_3 group, although less pronounced (δ_C = 42.2 and 35 ppm, respectively). However, the quaternary carbon directly bound to the variable substituent (C_{trz}–R) is oppositely polarized and hence, appears at lower field in complex **6** (R = OEt, δ_C = 157.6 ppm) than in complex **4a** (R = COOEt, δ_C = 137.2 ppm). The strong influence of the triazolylidene substituent is also supported by a shift of the N–CH_3 group in the ^1H NMR spectra which is increasingly shielded with stronger donating substituents R from δ_H = 4.12 (R = COOEt) to 3.90 (R = *n*Pr) and 3.70 (R = OEt). Remarkably, the chemical shift of the hydride *trans* to pyridine shows a correlation with the electronic nature of the triazolylidene substituents. A higher field shift was noted upon increasing

the electron donating character of the substituent R along the series with δ_H = –19.85 (**4a**, R = COOEt) > –20.04 (**5**, R = *n*Pr) > –20.16 ppm (**6**, R = OEt). Notably, the influence is weaker for the hydride ($\Delta\delta$ = 0.31 ppm) than for the NCH_3 group ($\Delta\delta$ = 0.42 ppm). Moreover, no such trend was observed for the chemical shift of the hydride *trans* to the carbene carbon and the phosphorus resonances. These resonances appear further downfield for complex **5** (δ_H = –10.95, δ_P = 19.7) than for complex **4a** (δ_H = –11.08, δ_P = 19.5) and are most upfield for complex **6** (δ_H = –11.52, δ_P = 18.9). This sequence does not reflect the electron-donating nature of the triazolylidene substituent and counteracts the general principle that the *trans* influence is much stronger than the *cis* influence. Possibly, other factors such as steric or polarity effects, are relevant for defining the shift of the resonances of these nuclei.

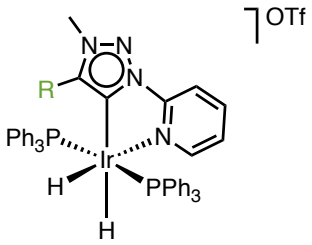

4a R = COOEt
5 R = $CH_2CH_2CH_3$
6 R = OEt

Figure 2. Complexes **4a**, **5** and **6** with different modifications on the triazole heterocycle.

Table 1. Selected chemical shifts from ^1H, ^{13}C and ^{31}P NMR analysis for complexes **4a**–**c**, **5** and **6**.[a]

Complex	^1H NMR (ppm)[b]			^{13}C NMR (ppm)				^{31}P NMR (ppm)
	NCH_3	H_{trans}	H_{cis}	C_{trz}–Ir	NCH_3	C_{trz}–R	C_{py}–N_{trz}	
4a	4.12	–11.08	–19.85	175.0	42.2	137.2	150.6	19.5
4b	4.09	–11.27	–19.95	173.0	42.0	137.1	144.2	20.0
4c	4.09	–11.14	–20.11	175.6	42.2	137.2	152.1	19.7
5	3.90	–10.95	–20.04	165.0	38.0	148.2	151.5	19.7
6	3.70	–11.52	–20.16	146.0	35.0	157.6	151.3	18.9

[a] in CD_3CN at 400 (^1H), 100 (^{13}C) and 121 (^{31}P) MHz; [b] *trans* and *cis* relative to the triazolylidene C_{trz}.

An analogous comparison of the spectroscopic properties of complexes **4a**–**c** allows for evaluating the influence of the substituents on the pyridine heterocycle (Table 1). According to ^{13}C NMR spectroscopy, the chemical shift of the carbenic carbon (Ir–C_{trz}) is similar for complexes **4a** and **4c** at 175.3(3) ppm, whereas it is slightly upfield shifted in complex **4b** (δ_C = 173 ppm). The quaternary pyridyl carbon bound to the triazole nitrogen (C_{py}–N_{trz}) also shifts remarkably (δ_C = 144.2 ppm for complex **4b** *vs.* 150.6 ppm for complex **4a** and 152.1 ppm for complex **4c**).

The upfield shifts of the C_{trz}–Ir and C_{py}–N_{trz} nuclei in complex **4b** are related to the *para* position of the –OMe group relative to the quaternary C_{py}. In contrast, the *meta* effect of the –OMe group in complex **4c** induces a downfield shift to δ_C = 152.1 ppm of this quaternary carbon.

The introduction of a –OMe substituent, either *para* or *meta* to the pyridyl nitrogen also shifts the two hydride resonances to higher field compared to the unsubstituted pyridyl system in complex **4a**. The changes are relatively small, however ($\Delta\delta$ 0.19 ppm for H_{trans} and 0.26 for H_{cis}). The methoxy substituent *para* to the pyridyl nitrogen in **4c** exerts a stronger shift of the hydride *trans* to the pyridyl nitrogen (H_{cis} δ_H = –20.11 *vs.* –19.85 for **4a**), than H_{trans} (δ_H = –11.14 *vs.* –11.08). In contrast, positioning the –OMe substituent *meta* to the pyridyl nitrogen (**4b**) affects the hydride *trans* to the carbene more (δ_H = –11.27 *vs.* –11.08), while the hydride *trans* to the pyridyl (H_{cis}) is less affected (δ_H = –19.95 *vs.* –19.85). Albeit small, these chemical shifts of the hydride correlate with the Hammett *meta* and *para* effects of the –OMe group (σ_{meta} = +0.12, σ_{para} = –0.27). Accordingly, the hydride *trans* to pyridine is directly influenced by the *para* effect of the OMe substituent in complex **4c** (σ_{para} = –0.27) and shows the highest shift of the series ($\delta_{H(cis)}$ = –20.11). A similar behavior of the OMe substituent can be surmised for complex **4b**, which is located in *para* position of the triazolylidene ring, and hence, the hydride *trans* to carbene carbon shows the highest shift of the series ($\delta_{H(trans)}$ = –11.27).

Structural characterization in the solid state. The structures of complexes **4a**–**c**, **5** and **6** were determined in the solid state by single crystal X-ray diffraction analyses and unambiguously confirmed the connectivity pattern deduced from NMR spectroscopy (Figure 3). All complexes feature an octahedral iridium center with two mutually *trans* positioned phosphines.[18,20] The Ir–H distances were refined with a constrained Ir–H distance to avoid divergence. Bond lengths and angles (Table 2) are generally within expectation and similar to related imidazolylidene complexes.[18,20] It is worth noting that the presence of the –OMe substituent on the pyridine induces an elongation of the Ir–N_{py} bond from 2.153(2) Å in **4a** to 2.187(±0.006) Å in complexes **4b** and **4c**. Moreover, the phosphines are considerably more linear in complex **6** containing an –OEt substituent on the triazolylidene unit (P1–Ir–P2 = 172°) than in the other complexes investigated here (P1–Ir–P2 = 165(±1)°) or reported in the literature (P1–Ir–P2 = 159°).[20]

The ester group in complexes **4a**–**c** is essentially co-planar with the triazolylidene heterocycle. In this series the *C*,*N*-bidentate ligand is wagging and variations in the Ir–C_{trz} bond length are compensated by a reciprocal modulation of the Ir–N_{py} distance. For example, complex **4a** has the longest Ir–C_{trz} bond and the shortest Ir–N_{py} bond of the series, while complex **4b** bearing –OMe *meta* to the N_{py} features the longest Ir–N_{py} and the shortest Ir–C_{trz} bond of the three complexes **4a**–**c** (Figure S3). Interestingly, the variation of Ir–C_{trz} bond length correlates well with the ^{1}H NMR chemical shift of the hydride *trans* to the Ir–C_{trz} bond. Thus, complex **4b** has the shortest

Ir–C_{trz} distance (2.050(5) Å) and the most hydridic hydride *trans* to the carbene carbon of the **4a**–**c** series (δ_H = –11.27). Complex **4c** is intermediate (Ir–C_{trz} = 2.059(6) Å, δ_H = –11.14) and complex **4a** with the longest Ir–C_{trz} bond (2.075(3) Å) shows the least hydridic *trans* hydride of the series (δ_H = –11.08). The direct response of both the Ir–C_{trz} bond length and the H_{trans} chemical shift upon introduction of electron donating substituents on the pyridine suggest a rational tunability of the electronic configuration of the metal center and the hydricity of the iridium-bound hydrogen.[21]

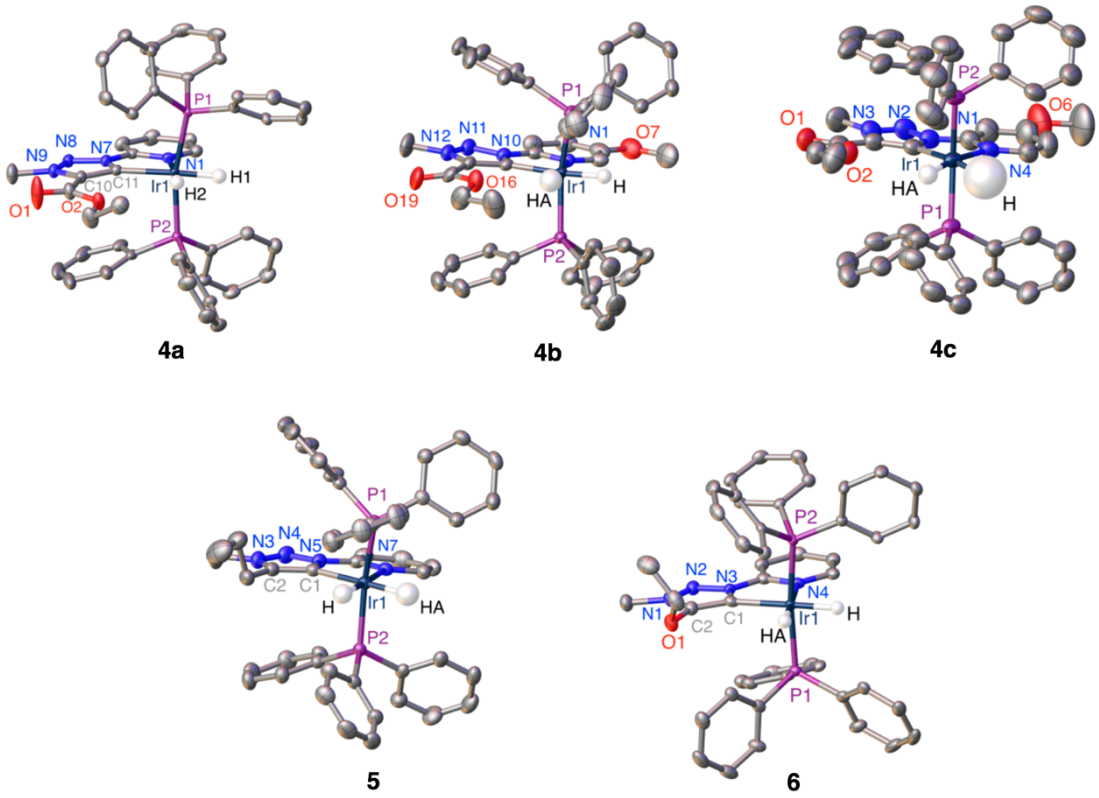

Figure 3. ORTEP plots for complexes **4a**–**c**, **5** and **6** (50% probability, non-coordinating anions and co-crystallized solvent molecules omitted for clarity). Only the metal bound hydrogens (calculated positions) are shown.

Table 2. Selected bond lengths (Å) and angles (°) for complexes **4a**–**c**, **5** and **6**.

Complex	**4a**	**4b**	**4c**	**5**	**6**
Ir–P1	2.2987(7)	2.2937(14)	2.2936(17)	2.2960(6)	2.2983(8)
Ir–P2	2.3048(7)	2.2846(13)	2.2874(17)	2.2998(6)	2.3115(7)
Ir–N_{py}	2.153(2)	2.193(5)	2.180(7)	2.1918(18)	2.177(3)
Ir–C_{trz}	2.075(3)	2.050(5)	2.059(6)	2.054(2)	2.095(3)
C_{trz}–C_{trz}	1.394(4)	1.389(8)	1.383(9)	1.385(3)	1.380(5)
C_{trz}–Ir–N_{py}	77.699(10)	77.662(2)	77.589(2)	77.090(8)	77.093(11)
P1–Ir–P2	165.752(2)	164.466(5)	165.850(7)	165.768(2)	172.563(3)

Kinetic hydricity of complex 4a upon reaction with different acids. While many iridium(III) dihydride systems are known,[22] only a much smaller number have the two hydrides in chemically inequivalent cis positions that have the potential to impart unique reactivity.[23,24] Due to the large inequivalence of the two hydrides in the iridium complexes **4**–**6**, the hydricity of complex **4a** was evaluated upon reaction with a variety of acids with different pK_a values (Scheme 2). These experiments were generally performed using an excess of the corresponding acid (200 eq) in $CDCl_3$ solution and using complex **4a** as the hydride source. Protonation involved selectively the hydride *trans* to the triazolylidene ligand and afforded the monohydride complexes **7**–**10**. The residual hydride *trans* to the pyridyl ligand appeared as a triplet at δ_H = –16.8(±0.4) ppm in complexes **7**–**10**, which corresponds to a downfield shift compared to the starting material by about 4 ppm (see also X-ray structures below). Diagnostically, also the ^{31}P NMR resonance shifts upfield from about 19 ppm in the dihydride complexes to 6.5(±1) ppm in the monohydride complexes **8**–**10**. The resonance is shifted to even higher field when phosphoric acid was used with δ_P = 0 ppm for complex **7**.

Scheme 2. Reaction of complex **4a** with a variety of acids with different pK_a.

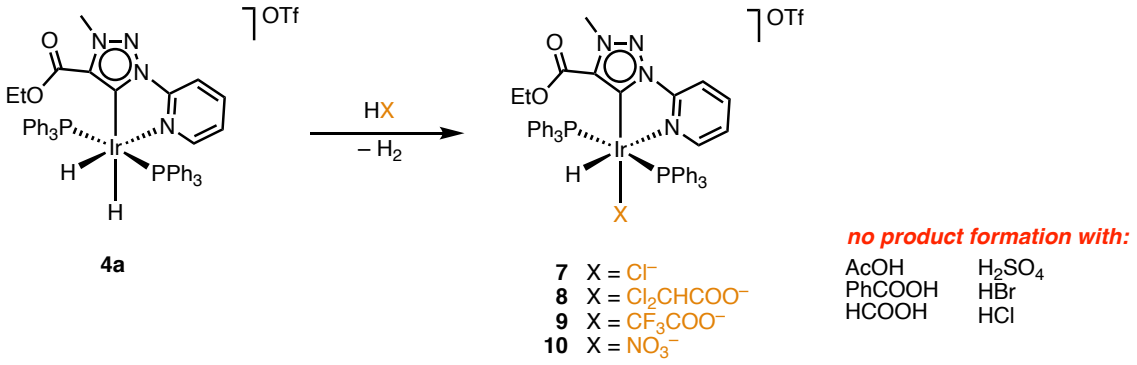

No reaction of **4a** took place under the standard conditions upon exposing this complex to weak acids such as formic acid (pK_a = 3.75), benzoic acid (pK_a = 4.20) or acetic acid (pK_a = 4.75) neither at room temperature nor at elevated temperature (70 ºC in $CDCl_3$; pK_a values in water, though a similar relative acidity trend is assumed in $CDCl_3$). Complete disappearance of the hydride resonance was observed with phosphoric acid (pK_a = 2.12) after 38 h at 70 ºC as well as with dichloroacetic acid (pK_a = 1.35, full conversion after 20 h). With oxalic acid (pK_a = 1.21) the reaction ceased after about 20% conversion, suggesting some undesired side-reactions of this acid. Complex **4a** reacted significantly faster with trifluoroacetic acid (pK_a = 0.25) and was fully consumed after 5 min already at room temperature. With stronger acids, divergent reactivity patterns were observed (see SI for details).

It is worth noting that the electronically more *deshielded* hydride at δ_H = –11 ppm and *trans* to the carbene is reacting with the acid as it disappears over time or instantly depending on the acid

used, and not the hydrogen *trans* to the pyridyl unit that is more hydridic according to its NMR chemical shift (δ_H = –20 ppm). This hydride however changes multiplicity from a doublet of triplets to a simple triplet and disappears over time with concomitant growing of the signal around δ_H = –17 ppm indicative of the new monohydride complexes. The high selectivity of the reaction indicates that the *trans* effect (carbene > pyridine) is more relevant than the hydricity deduced from NMR spectroscopy, in agreement with kinetic rather than thermodynamic hydricity governing the reactivity pathway.[14,25,26] Moreover, the reactivity of the hydride is correlated to the acid strength only within a limited pK_a window in the 0–5 range. With stronger acids the reactivity is highly diverging and may involve the reaction of both hydrides and maybe reactions including reductive elimination and oxidative addition cycles. An unaccounted outlier is nitric acid (pK_a = –1.4) which needs elevated temperature to selectively form one product, while trifluoroacetic acid (pK_a = 0.25) reacts instantly at room temperature.[27]

The striking difference of the two hydrides in complexes **4a** is remarkable, especially when considering that related complexes with inequivalent *cis* dihydride ligands showed either rapid exchange in the presence upon protonation, or the reactivity of the hydrides is not known.[23] A complex with a *C,N*-bidentate benzoquinone *trans* to the two hydrides showed exclusive reactivity of one hydride, though only when a directing ammonium group was present in close proximity to the hydride *trans* to the aryl donor site.[24]

No reactivity of complex **4a** towards peroxides (H_2O_2 and ^{t}BuOOH) was observed. Although peroxides in presence of CuI reacted with complex **4a** at room temperature within 5 min to give the iodide complex **11** (Scheme 3). This iodide complex was characterized by a high-field phosphine resonance (δ_P = –4.7 ppm) and a hydride resonance that is less downfield (δ_H = –17.93 ppm) than the hydrides of complexes **8**–**10** containing oxo acid fragments. Similar reactivity patterns were observed also when complex **4a** was reacted with *meta*-chloroperoxybenzoic acid (*m*CPBA), which formed the benzoate complex **12** at room temperature within 10 min (Scheme 3). Both products where further identified by a single crystal X-ray diffraction analysis.

Scheme 3. Synthesis of complexes **11** and **12** from complex **4a** and ORTEP plots for both complexes (50% probability, H atoms except hydrides, non-coordinating anions and co-crystallized solvent omitted for clarity).

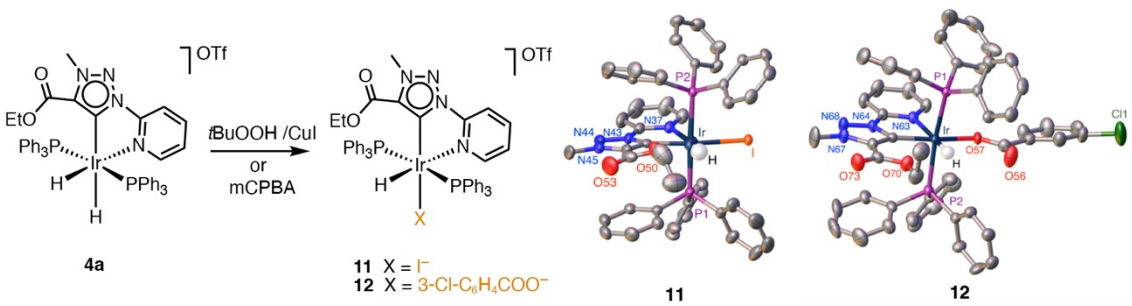

Hydricity of complexes 4–6. More detailed insights into the reactivity of these complexes were obtained by kinetic measurements using dichloroacetic acid. The addition of an excess of this acid (200 molar equivalents, pseudo-first order conditions) to a solution of the metal complexes resulted in the clean formation of the corresponding monohydride complexes **8**, **13** and **14** (Scheme 4).

Scheme 4. Reaction of complex **4**–**6** with dichloroacetic acid.

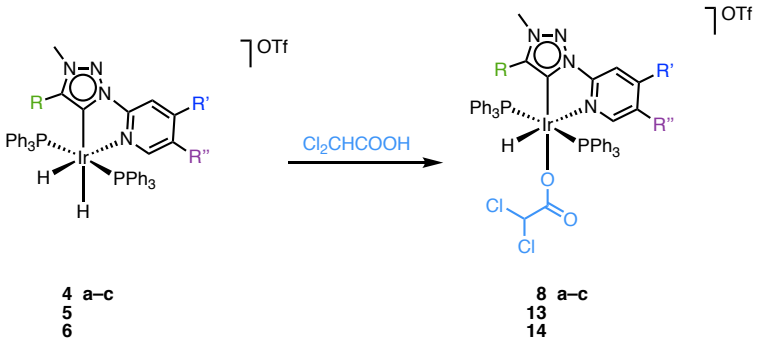

4 a–c
5
6

8 a–c
13
14

The reactivity of the different complexes was studied by NMR spectroscopic monitoring of the disappearance of the dihydride complexes **4**–**6** (δ_H –20, δ_P 19) and the gradual formation of the monohydride product around (δ_H –16, δ_P 6) using a capillary containing a known ruthenium(II) phosphine hydride complex as internal standard. We noted that the hydride *trans* to the carbene carbon resonance rapidly disappears after adding dichloroacetic acid, probably due to isotope exchange, since all other ^{1}H NMR signals are preserved without any change of resonance frequency. Both the ^{1}H and the ^{31}P NMR probes consistently indicate that complexes **4c** and **5** are the most reactive complexes with dichloroacetic acid at 70 ºC and reach full conversion within 5 h (Figure 7a, Fig. S4). Logarithmic plots of the concentration of the dihydride complex *versus* time showed a linear correlation, indicating (pseudo-)first-order kinetics with k_{obs} = 183(±17) × 10^{-6} s^{-1} and 193(±7) × 10^{-6} s^{-1} for **4c** and **5**, respectively (Fig. 7b). Complex **4a** is less reactive and needs 20 h to fully transform the dihydride complex (k_{obs} = 56(±3) × 10^{-6} s^{-1}). In contrast, complexes **4b** and **6** were not fully converted and reached about 75% conversion after 20 h with the lowest observed rates of this series, k_{obs} = 15(±4) and 25(±6) × 10^{-6} s^{-1}, respectively.[28]

It is interesting to note that these rates do not correlate with the electronic impact of the triazolylidene ligand. Thus, the alkyl-substituted triazolylidene in complex **5** imparts almost an order of magnitude higher reactivity towards the acid than complex **6** with an electron-donating alkoxy substituent, while the analogous complex **4a** with an electron-withdrawing ester unit has intermediate reactivity. In contrast, the pyridyl substitution appears more rational with para-OMe substitution with a negative Hammett parameter (σ_p = –0.27, **4c**) inducing faster rates than no

substituent ($\sigma = 0$, **4a**), while the meta-OMe system is the slowest ($\sigma_m = +0.12$, **4b**). This trend is remarkable, since the pyridyl substituent is *cis* to the supposedly most reactive hydride.

Moreover, the hydricity deduced by ^{1}H NMR spectroscopy is not correlated to the reactivity rates (Fig. S5). For example, complex **6** containing the most hydridic hydride *trans* to the carbene carbon (δ_H –11.52) has a very low reaction rate ($k_{obs} = 25 \times 10^{-6}$ s^{-1}), whereas the fastest reacting complexes, **4c** and **5**, feature hydrides with intermediate or lowest field chemical shifts in this series (δ_H –11.14 and –10.95, respectively). This work therefore indicates that the NMR-deduced hydricity is not a valuable proxy for predicting the reactivity in these dihydride complexes **4–6** and that instead other factors may be relevant for imparting high reactivity, such as heteroatom-induced hydride or proton stabilization.

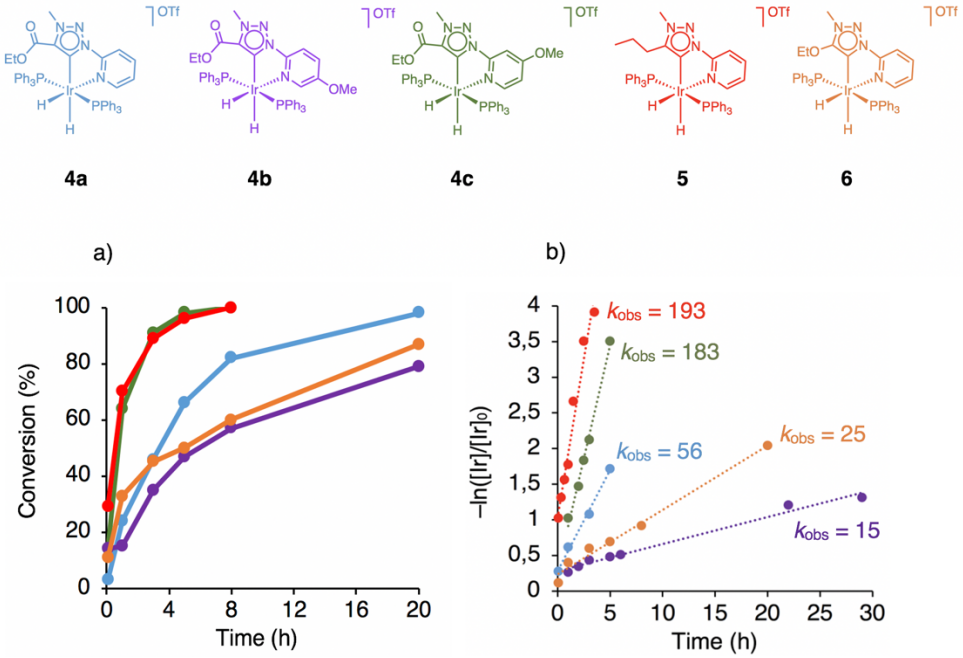

Figure 4. For complexes **4a** (blue), **4b** (purple), **4c** (green), **5** (red) and **6** (orange). a) Time-dependent conversion profile for the reaction of each complex with $Cl_2CHCOOH$. Conditions: $Cl_2CHCOOH$ (200 eq), [Ir] (4 µmol), $CDCl_3$ (0.4 mL), 70 ºC. Conversions were determined by ^{31}P NMR integration following the disappearance of the triphenylphosphine resonance ($\delta_P \sim 19$ ppm using a phosphine Ru complex as internal standard; see experimental section for further details). b) Log-scale of the time-dependent change of the relative concentration for each dihydride complex monitored by ^{31}P NMR spectroscopy. $[Ir]_0$ refers to the initial concentration of the dihydride complex and [Ir] to the concentration of this complex at the corresponding reaction time, k_{obs} values as 10^{-6} s^{-1}.

Conclusion

A new family of pyridyl-carbene iridium(III) complexes bearing hydride ligands has been successfully prepared. The hydride reactivity towards different acids within a large range of pK_a

values has been evaluated and showed to be dependent on the acid strength within a limited range (pK_a between 0–5). The hydride reactivity is influenced by the *trans* effect (carbene > pyridine) rather than the hydridic character determined by NMR chemical shift comparison. While modulation of the electronic properties of the carbene ligand site did not show any correlation with the reactivity of the hydrides, substitution of the pyridyl unit affected the reactivity of the *cis* hydride, *i.e.* the hydride located *trans* to the carbene carbon. Only the hydride *trans* to the carbene carbon was exchanged selectively, even in the presence of a large excess of acids, which may become an attractive feature for catalytic applications.

Experimental section

General. Ligands **1**–**3** and $IrH_5(PPh_3)_2$ were prepared according to literature methods;[16,17,29] all other reagents and solvents were used as obtained from commercial suppliers. Unless specified, NMR spectra were recorded at 25 °C on Bruker spectrometers operating at 300 or 400 MHz (^{1}H NMR), 100 MHz (^{13}C NMR), and 121 MHz (^{31}P NMR) respectively. Chemical shifts (δ in ppm, coupling constants J in Hz) were referenced to residual solvent resonances (^{1}H, ^{13}C). Assignments are based on homo- and heteronuclear shift correlation spectroscopy. All complexes show a quartet around 120 ppm in the ^{13}C NMR spectrum due to the OTf counterion. Purity of the complexes has been established by NMR spectroscopy, and by elemental analysis, which were performed by the University of Bern Microanalytic Laboratory using a Thermo Scientific Flash 2000 CHNS-O elemental analyzer. High-resolution mass spectrometry was carried out with a Thermo Scientific LTQ Orbitrap XL (ESI-TOF).

General procedure for the synthesis of complexes 4–6: A mixture of the pyridyl-triazolium salt (1 eq) and $IrH_5(PPh_3)_2$ (1 eq) in toluene (15 mL) was refluxed for 24 h. The solvent was removed under reduced pressure and the residue was dissolved in CH_2Cl_2 and layered with Et_2O to induce precipitation of a light yellow solid, which was collected by decantation and dried in vacuo to afford the title complex. The complex was purified *via* column chromatography (SiO_2; CH_2Cl_2/acetone, 50:0 to 50:15 gradient).

Complex 4a. A mixture of **1a** (53 mg, 0.14 mmol) and $IrH_5(PPh_3)_2$ (100 mg, 0.14 mmol) in toluene (15 mL) was refluxed for 24 h according to the general procedure to obtain complex **4a**. Yield: 73 mg (47%). ^{1}H NMR (400 MHz, CD_3CN): δ = 8.29 (d, $^3J_{HH}$ = 5.4 Hz, 1H, H_{py}), 7.89–7.81 (m, 1H, H_{py}), 7.72 (d, $^3J_{HH}$ = 7.8 Hz, 1H, H_{py}), 7.50–7.21 (m, 30H, H_{Ph}), 6.90 (ddd, $^3J_{HH}$ = 7.8 Hz, $^3J_{HH}$ = 5.4 Hz, $^5J_{HH}$ = 1.2 Hz, 1H, H_{py}), 4.20 (q, $^3J_{HH}$ = 7.2 Hz, 2H, OCH_2Me), 4.12 (s, 3H, NCH_3), 1.19 (t, $^3J_{HH}$ = 7.2 Hz, 3H, OCH_2CH_3), –11.08 (dt, $^2J_{PH}$ = 17.0 Hz, $^2J_{HH}$ = 5.9 Hz, 1H, Ir–H), –19.85 (dt, $^2J_{PH}$ = 17.0 Hz, $^2J_{HH}$ = 5.9 Hz, 1H, Ir–H). ^{13}C{^{1}H} NMR (100 MHz, CD_3CN):

δ = 175.0 (t, J_{PC} = 5.7 Hz, C_{trz}–Ir), 158.9 (C=O), 156.7 (C_{py}H), 150.6 (C_{py}–N_{trz}), 140.9 (C_{py}H), 137.2 (C_{trz}–COOEt), 134.3 (t, J_{PC} = 27.4 Hz, C_{Ph}), 134.1 (t, J_{PC} = 6.2 Hz, C_{Ph}), 131.2 (C_{Ph}), 129.1 (t, J_{PC} = 5.0 Hz, C_{Ph}), 127.0 (C_{py}H), 115.0 (C_{py}H), 62.9 (OCH_2Me), 42.2 (NCH_3), 14.3 (OCH_2CH_3). $^{31}P\{^1H\}$ NMR (121 MHz, CD_3CN): δ = 19.5. Anal. Calcd for $C_{48}H_{44}F_3IrN_4O_5P_2S$ (1100.12): C, 52.41; H, 4.03; N, 5.09. Found: C, 52.40; H, 3.60; N, 5.36 HR-MS (CH_3CN): m/z calculated for $C_{47}H_{44}O_2N_4IrP_2$ $[M–OTf]^+$ = 951.2563; found, 951.2552.

Complex 4b. A mixture of **1b** (57.1 mg, 0.14 mmol) and $IrH_5(PPh_3)_2$ (100 mg, 0.14 mmol) in toluene (15 mL) was refluxed for 24 h according to the general procedure yielding complex **4b**. Yield: 61 mg (39%). ^1H NMR (400 MHz, CD_3CN): δ = 7.68–7.60 (m, 2H, H_{py}), 7.53–7.43 (m, 13H, H_{Ph}+ H_{py}), 7.39–7.22 (m, 18H, H_{Ph}), 4.24 (q, $^3J_{HH}$ = 7.2 Hz, 2H, OCH_2Me), 4.09 (s, 3H, NCH_3), 3.60 (s, 3H, OCH_3), 1.23 (t, $^3J_{HH}$ = 7.2 Hz, 3H, OCH_2CH_3), –11.27 (td, $^2J_{PH}$ = 17.0 Hz, $^2J_{HH}$ = 6.0 Hz, 1H, Ir–H), –19.95 (td, $^2J_{PH}$ = 17.0 Hz, $^2J_{HH}$ = 6.0 Hz, 1H, Ir–H). $^{13}C\{^1H\}$ NMR (100 MHz, CD_3CN): δ = 173.0 (t, J_{PC} = 6.3 Hz, C_{trz}–Ir), 159.0 (C=O), 157.9 (C_{py}–OMe), 144.2 (C_{py}–N_{trz}), 142.2 (C_{py}H), 137.1 (C_{trz}–COOEt), 134.3 (t, J_{PC} = 27.4 Hz, C_{Ph}), 134.1 (t, J_{PC} = 6.2 Hz, C_{Ph}), 131.2 (C_{Ph}), 129.1 (t, J_{PC} = 5.0 Hz, C_{Ph}), 126.3 (C_{py}H), 115.7 (C_{py}H), 62.9 (OCH_2Me), 57.4 (OCH_3), 42.0 (NCH_3), 14.3 (OCH_2CH_3). $^{31}P\{^1H\}$ NMR (121 MHz, CD_3CN): δ = 20.0. Anal. Calcd for $C_{49}H_{46}F_3IrN_4O_6P_2S$ (1130.15): C, 52.08; H, 4.10; N, 4.96. Found: C, 52.60; H, 3.72; N, 4.77. HR-MS (CH_3CN): m/z calculated for $C_{48}H_{46}O_3N_4IrP_2$ $[M–OTf]^+$ = 981.2669; found, 981.2671.

Complex 4c. A mixture of **1c** (57.1 mg, 0.14 mmol) and $IrH_5(PPh_3)_2$ (100 mg, 0.14 mmol) in toluene (15 mL) was refluxed for 24 h according to the general procedure affording complex **4c**. Yield: 47 mg (30%). ^1H NMR (400 MHz, CD_3CN): δ = 8.02 (d, $^3J_{HH}$ = 6.6 Hz, 1H, H_{py}), 7.54–7.43 (m, 12H, H_{Ph}), 7.40–7.30 (m, 18H, H_{Ph}), 7.18 (d, $^4J_{HH}$ = 2.6 Hz, 1H, H_{py}), 6.45 (dd, $^3J_{HH}$ = 6.6 Hz, $^4J_{HH}$ = 2.6 Hz, 1H, H_{py}), 4.20 (q, $^3J_{HH}$ = 7.2 Hz, 2H, OCH_2Me), 4.09 (s, 3H, NCH_3), 3.86 (s, 3H, OCH_3), 1.19 (t, $^3J_{HH}$ = 7.2 Hz, 3H, OCH_2CH_3), –11.14 (td, $^2J_{PH}$ = 17.0 Hz, $^2J_{HH}$ = 6.0 Hz, 1H, Ir–H), –20.10 (td, $^2J_{PH}$ = 17.0 Hz, $^2J_{HH}$ = 6.0 Hz, 1H, Ir–H). $^{13}C\{^1H\}$ NMR (100 MHz, CD_3CN): δ = 175.6 (t, J_{PC} = 5.4 Hz, C_{trz}–Ir), 169.1 (C_{py}–OMe), 158.9 (C=O), 157.0 (C_{py}H), 152.1 (C_{py}–N_{trz}), 137.2 (C_{trz}–COOEt), 134.5 (t, J_{PC} = 27.2 Hz, C_{Ph}), 134.1 (t, J_{PC} = 6.2 Hz, C_{Ph}), 131.1 (C_{Ph}), 129.1 (t, J_{PC} = 5.0 Hz, C_{Ph}), 113.7 (C_{py}H), 101.0 (C_{py}H), 62.9 (OCH_2Me), 57.7 (OCH_3), 42.2 (NCH_3), 14.3 (OCH_2CH_3). $^{31}P\{^1H\}$ NMR (121 MHz, CD_3CN): δ = 19.7. Anal. Calcd for $C_{49}H_{46}F_3IrN_4O_6P_2S$ (1130.15): C, 52.08; H, 4.10; N, 4.96. Found: C, 51.59; H, 3.85; N, 4.71. HR-MS (CH_3CN): m/z calculated for $C_{48}H_{46}O_3N_4IrP_2$ $[M–OTf]^+$ = 981.2669; found, 981.2676.

Complex 5. A mixture of **2** (48 mg, 0.13 mmol) and $IrH_5(PPh_3)_2$ (98.3 mg, 0.13 mmol) in toluene (15 mL) was refluxed for 24 h according to the general procedure affording complex **5**. Yield: 50

mg (36%).^{1}H NMR (400 MHz, CD_3CN): δ = 8.36 (d, $^{3}J_{HH}$ = 5.5 Hz, 1H, H_{py}), 7.73 (t, $^{3}J_{HH}$ = 8.0 Hz, 1H, H_{py}), 7.47 (d, $^{3}J_{HH}$ = 8.0 Hz, 1H, H_{py}), 7.43–7.22 (m, 30H, H_{Ph}), 6.92–6.84 (m, 1H, H_{py}), 3.90 (s, 3H, NCH_3), 2.08–2.01 (m, 2H, CH_2), 0.80–0.70 (m, 2H, CH_2), 0.66 (t, $^{3}J_{HH}$ = 7.0 Hz, 3H, CH_3), –10.95 (td, $^{2}J_{PH}$ = 17.0 Hz, $^{2}J_{HH}$ = 6 Hz, 1H, Ir–H), –20.04 (td, $^{2}J_{PH}$ = 17.0 Hz, $^{2}J_{HH}$ = 6 Hz, 1H, Ir–H). $^{13}C\{^{1}H\}$ NMR (100 MHz, CD_3CN): δ = 165.0 (t, J_{PC} = 6.9 Hz, C_{trz}–Ir), 156.5 ($C_{py}H$), 151.5 (C_{py}–N_{trz}), 148.2 (C_{trz}–$CH_2CH_2CH_3$), 140.4 ($C_{py}H$), 134.2 (t, J_{PC} = 26.9 Hz, C_{Ph}), 134.0 (t, J_{PC} = 6.1 Hz, C_{Ph}), 131.1 (C_{Ph}), 129.2 (t, J_{PC} = 5.0 Hz, C_{Ph}), 126.4 ($C_{py}H$), 114.8 ($C_{py}H$), 38.0 (NCH_3), 27.7 (CH_2), 21.8 (CH_2), 14.6 (CH_3). $^{31}P\{^{1}H\}$ NMR (121 MHz, CD_3CN): δ = 19.7. Anal. Calcd for $C_{50}H_{49}F_3IrN_5O_3P_2S$ + CH_3CN (1111.19): C, 54.05; H, 4.44; N, 6.30. Found: C, 54.52; H, 4.59; N, 6.66. HR-MS (CH_3CN): m/z calculated for $C_{47}H_{46}N_4IrP_2$ $[M–OTf]^+$ = 921.2827; found, 921.2837.

Complex 6. A mixture of **3** (49 mg, 0.14 mmol) and $IrH_5(PPh_3)_2$ (100 mg, 0.14 mmol) in toluene (15 mL) was refluxed for 24 h according to the general procedure affording complex **6**. Yield: 62 mg (41%). ^{1}H NMR (400 MHz, CD_3CN): δ = 8.30 (d, $^{3}J_{HH}$ = 5.5 Hz, 1H, H_{py}), 7.78–7.67 (m, 1H, H_{py}), 7.51 (d, $^{3}J_{HH}$ = 8.3 Hz, 1H, H_{py}), 7.45–7.16 (m, 30H, H_{Ph}), 6.93–6.81 (m, 1H, H_{py}), 3.87 (q, $^{3}J_{HH}$ = 7.2 Hz, 2H, OCH_2Me), 3.70 (s, 3H, NCH_3), 0.95 (t, $^{3}J_{HH}$ = 7.2 Hz, 3H, OCH_2CH_3), –11.52 (td, $^{2}J_{PH}$ = 17.0 Hz, $^{2}J_{HH}$ = 6.1 Hz, 1H, Ir–H), –20.16 (td, $^{2}J_{PH}$ = 17.0 Hz, $^{2}J_{HH}$ = 6.1 Hz, 1H, Ir–H). $^{13}C\{^{1}H\}$ NMR (100 MHz, CD_3CN): δ = 157.6 (C_{trz}–OEt), 156.4 ($C_{py}H$), 151.3 (C_{py}–N_{trz}), 146.0 (t, J_{PC} = 6.3 Hz, C_{trz}–Ir),140.4 ($C_{py}H$), 134.1 (t, J_{PC} = 26.09 Hz, C_{Ph}), 134.0 (t, J_{PC} = 6.2 Hz, C_{Ph}), 131.1 (C_{Ph}), 129.2 (t, J_{PC} = 5.0 Hz, C_{Ph}), 126.6 ($C_{py}H$), 114.6 ($C_{py}H$), 70.4 (OCH_2Me), 35.0 (NCH_3), 15.2 (OCH_2CH_3). $^{31}P\{^{1}H\}$ NMR (121 MHz, CD_3CN): δ = 18.89. Anal. Calcd for $C_{47}H_{44}F_3IrN_4O_4P_2S$ (1072.11): C, 52.65; H, 4.14; N, 5.23. Found: C, 52.40; H, 3.78; N, 5.07. HR-MS (CH_3CN): m/z calculated for $C_{46}H_{44}ON_4IrP_2$ $[M–OTf]^+$ = 923.2614; found, 923.2625.

General procedure for the reaction of complex 4a with acids. In a NMR tube, complex **4a** (1 eq) and an excess of the corresponding acid (200 eq) in $CDCl_3$ or CD_3CN (0.4 mL) was followed by ^{1}H and ^{31}P NMR spectroscopy until the reaction was finished. The reaction was carried out at room temperature or elevated temperature (70 ºC). The residue was layered with Et_2O to induce precipitation of a white solid, which was dried under reduced pressure to afford the title complex.

Complex 7. From **4a** (5 mg, 0.004 mmol) and phosphoric acid (60 μL, 0.87 mmol) in $CDCl_3$ (0.4 mL) after 38 h at 70 ºC. ^{1}H NMR (400 MHz, CD_3CN): δ = 9.12 (d, $^{3}J_{HH}$ = 5.4 Hz, 1H, H_{py}), 8.10 (t, $^{3}J_{HH}$ = 8.4 Hz, 1H, H_{py}), 8.06 (d, $^{3}J_{HH}$ = 8.4 Hz, 1H, H_{py}), 7.56–7.50 (m, 1H, H_{py}), 7.47–7.24 (m, 30H, H_{Ph}), 4.01–3.88 (m, 2H, OCH_2Me), 3.98 (s, 3H, NCH_3), 1.31 (t, $^{3}J_{HH}$ = 7.2 Hz, 3H, OCH_2CH_3), –17.25 (t, $^{2}J_{PH}$ = 14.1 Hz, 1H, Ir–H). $^{13}C\{^{1}H\}$ NMR (100 MHz, CD_3CN): δ = 156.8 (C=O), 152.7 (t, C_{trz}–Ir), 151.7 ($C_{py}H$), 149.4 (C_{py}–N_{trz}), 142.6 ($C_{py}H$), 134.8 (C_{trz}–COOEt), 134.5

(t, J_{PC} = 5.6 Hz, C_{Ph}), 131.9 (C_{Ph}), 131.4 (t, J_{PC} = 27.7 Hz, C_{Ph}), 129.2 (t, J_{PC} = 5.0 Hz, C_{Ph}), 127.5 ($C_{py}H$), 115.1 ($C_{py}H$), 63.1 (OCH_2Me), 43.3 (NCH_3), 14.4 (OCH_2CH_3). $^{31}P\{^1H\}$ NMR (121 MHz, CD_3CN): δ = 0. HR-MS (CH_3CN): m/z calculated for $C_{47}H_{43}ClIrN_4O_2P_2$ $[M–OTf]^+$ = 985.2179; found, 985.2155.

Complex 8. From **4a** (5 mg, 0.004 mmol) and dichloroacetic acid (72 µL, 0.87 mmol) in $CDCl_3$ (0.4 mL) after 20 h at 70 ºC. ^1H NMR (400 MHz, CD_3CN): δ = 9.26 (d, $^3J_{HH}$ = 5.5 Hz, 1H, H_{py}), 8.05 (t, $^3J_{HH}$ = 8.0 Hz, 1H, H_{py}), 7.73–7.68 (m, 1H, H_{py}), 7.62 (d, $^3J_{HH}$ = 8.0 Hz, 1H, H_{py}), 7.49–7.28 (m, 30H, H_{Ph}), 5.5 (s, 1H, $CHCl_2$), 4.1 (s, 3H, NCH_3), 4.03 (q, $^3J_{HH}$ = 7.2 Hz, 2H, OCH_2Me), 1.26 (t, $^3J_{HH}$ = 7.2 Hz, 3H, OCH_2CH_3), –16.64 (t, $^2J_{PH}$ = 13.3 Hz, 1H, Ir–H). $^{13}C\{^1H\}$ NMR (100 MHz, CD_3CN): δ = 168.1 (Cl_2CHC=O), δ = 157.4 (C=O), 151.3 ($C_{py}H$), 148.8 (C_{py}–N_{trz}), 147.9 (C_{trz}–Ir), 142.7 ($C_{py}H$), 136.2 (C_{trz}–COOEt), 134.3 (t, J_{PC} = 5.8 Hz, C_{Ph}), 131.9 (C_{Ph}), 129.8 (t, J_{PC} = 27.6 Hz, C_{Ph}), 129.4 (t, J_{PC} = 5.1 Hz, C_{Ph}), 127.6 ($C_{py}H$), 115.3 ($C_{py}H$), 67.5 (Cl_2CH), 63.4 (OCH_2Me), 42.9 (NCH_3), 14.6 (OCH_2CH_3). $^{31}P\{^1H\}$ NMR (121 MHz, CD_3CN): δ = 5.6. HR-MS (CH_3CN): m/z calculated for $C_{49}H_{44}Cl_2IrN_4O_4P_2$ $[M–OTf]^+$ = 1077.1844; found, 1077.1839.

Complex 9. From **4a** (5 mg, 0.004 mmol) and trifluoroacetic acid (67 µL, 0.87 mmol) in $CDCl_3$ (0.4 mL) after 5 min at room temperature. ^1H NMR (400 MHz, CD_3CN): δ = 9.18 (d, $^3J_{HH}$ = 5.5 Hz, 1H, H_{py}), 8.10–7.96 (m, 1H, H_{py}), 7.75–7.66 (m, 1H, H_{py}), 7.60 (d, $^3J_{HH}$ = 8.2 Hz, 1H, H_{py}), 7.47–7.25 (m, 30H, H_{Ph}), 4.11 (s, 3H, NCH_3), 4.06 (q, $^3J_{HH}$ = 7.1 Hz, 2H, OCH_2Me), 1.27 (t, $^3J_{HH}$ = 7.1 Hz, 3H, OCH_2CH_3), –16.61 (t, $^2J_{PH}$ = 13.2 Hz, 1H, Ir–H). $^{13}C\{^1H\}$ NMR (100 MHz, $CDCl_3$): δ = 207.1 (CF_3C=O), 156.6 (C=O), 148.9 (C_{py}–N_{trz}), 148.1 ($C_{py}H$), 146.6 (C_{trz}–Ir), 142.6 ($C_{py}H$), 134.9 (C_{trz}–COOEt), 133.3 (t, J_{PC} = 5.7 Hz, C_{Ph}), 131.3 (C_{Ph}), 128.6 (t, J_{PC} = 5.1 Hz, C_{Ph}), 128.3 (t, J_{PC} = 27.7 Hz, C_{Ph}), 126.1 ($C_{py}H$), 116.0 (CF_3), 62.5 (OCH_2Me), 42.6 (NCH_3), 14.2 (OCH_2CH_3), one C_{py} not resolved. $^{31}P\{^1H\}$ NMR (121 MHz, CD_3CN): δ = 6.4. HR-MS (CH_3CN): m/z calculated for $C_{49}H_{43}F_3IrN_4O_4P_2$ $[M–OTf]^+$ = 1063.2341; found, 1063.2338.

Complex 10. From **4a** (5 mg, 0.004 mmol) and nitric acid (62 µL, 0.87 mmol) in $CDCl_3$ (0.4 mL) after 15 min at 70 ºC. ^1H NMR (300 MHz, CD_3CN): δ = 9.07 (d, $^3J_{HH}$ = 5.5 Hz, 1H, H_{py}), 8.04 (td, $^3J_{HH}$ = 8.0 Hz, $^3J_{HH}$ = 1.6 Hz 1H, H_{py}), 7.68–7.58 (m, 2H, H_{py}), 7.50–7.27 (m, 30H, H_{Ph}), 4.12 (q, $^3J_{HH}$ = 7.2 Hz, 2H, OCH_2Me), 4.10 (s, 3H, NCH_3), 1.30 (t, $^3J_{HH}$ = 7.2 Hz, 3H, OCH_2CH_3), –16.38 (t, $^2J_{PH}$ = 12.8 Hz, 1H, Ir–H). $^{31}P\{^1H\}$ NMR (121 MHz, CD_3CN): δ = 7.4. HR-MS (CH_3CN): m/z calculated for $C_{47}H_{43}IrN_5O_5P_2$ $[M–OTf]^+$ = 1012.2374; found, 1012.2361.

Complex 11. From **4a** (5 mg, 0.004 mmol), with H_2O_2 (10 µL, 0.28 mmol) and CuI (2 mg, 0.010 mmol) in $CDCl_3$ (0.4 mL) after 5 min at room temperature. ^1H NMR (400 MHz, CD_3CN): δ =

9.37 (d, $^3J_{HH}$ = 5.4 Hz, 1H, H_{py}), 8.19 (t, $^3J_{HH}$ = 8.0 Hz, 1H, H_{py}), 8.11 (d, $^3J_{HH}$ = 8.0 Hz, 1H, H_{py}), 7.64–7.59 (m, 1H, H_{py}), 7.46–7.26 (m, 30H, H_{Ph}), 4.09 (q, $^3J_{HH}$ = 7.2 Hz, 2H, OCH_2Me), 3.97 (s, 3H, NCH_3), 1.40 (t, $^3J_{HH}$ = 7.2 Hz, 3H, OCH_2CH_3), –17.93 (t, $^2J_{PH}$ = 13.9 Hz, 1H, Ir–H). $^{13}C\{^1H\}$ NMR (100 MHz, CD_3CN): δ = 156.9 (C=O), 154.5 ($C_{py}H$), 154.3 (t, C_{trz}–Ir), 149.5 (C_{py}–N_{trz}), 142.9 ($C_{py}H$), 134.9 (t, J_{PC} = 5.4 Hz, C_{Ph}), 134.4 (C_{trz}–COOEt), 131.9 (t, J_{PC} = 28.1 Hz, C_{Ph}), 131.8 (C_{Ph}), 129.0 (t, J_{PC} = 5.1 Hz, C_{Ph}), 128.5 ($C_{py}H$), 115.6 ($C_{py}H$), 63.4 (OCH_2Me), 43.6 (NCH_3), 14.5 (OCH_2CH_3). $^{31}P\{^1H\}$ NMR (121 MHz, CD_3CN): δ = –4.7. HR-MS (CH_3CN): m/z calculated for $C_{47}H_{43}IIrN_4O_2P_2$ $[M–OTf]^+$ = 1077.1535; found, 1077.1533.

Complex 12. From **4a** (5 mg, 0.004 mmol) and *m*CPBA (1.7 mg, 0.01 mmol) in CD_3CN (0.4 mL) after 10 min reaction at room temperature. ^1H NMR (300 MHz, CD_3CN): δ = 9.35 (d, $^3J_{HH}$ = 5.5 Hz, 1H, H_{py}), 8.06 (td, $^3J_{HH}$ = 8.0 Hz, $^3J_{HH}$ = 1.5 Hz 1H, H_{py}), 7.80–7.67 (m, 1H, H_{py}), 7.61 (d, $^3J_{HH}$ = 8.0 Hz, 1H, H_{py}), 7.54–7.44 (m, 4H, H_{ClPh}), 7.42–7.14 (m, 30H, H_{Ph}), 4.10 (s, 3H, NCH_3), 4.07 (q, $^3J_{HH}$ = 7.2 Hz, 2H, OCH_2Me), 1.27 (t, $^3J_{HH}$ = 7.2 Hz, 3H, OCH_2CH_3), –16.67 (t, $^2J_{PH}$ = 13.2 Hz, 1H, Ir–H). $^{31}P\{^1H\}$ NMR (121 MHz, CD_3CN): δ = 6.8. HR-MS (CH_3CN): m/z calculated for $C_{54}H_{47}ClIrN_4O_4P_2$ $[M–OTf]^+$ = 1105.2390; found, 1105.2409.

Kinetic experiments: Kinetic measurements were performed at 70 °C in a 300 MHz NMR spectrometer with the corresponding iridium complex (10 mM in $CDCl_3$) using as internal standard a glass capillary containing the ruthenium phosphine hydride complex $[RuH(CO)(C,N)(PPh_3)_2]OTf$ (C,N = triazolylidene-pyridyl ligand as in complex **4b**; Fig. S6) dissolved in $CDCl_3$.

Crystal structure determination. All measurements were made on an Oxford Diffraction SuperNova area-detector diffractometer[30] using mirror optics monochromated Mo *K*α radiation (λ = 0.71073 Å) and Al filtered.[31] Data reduction was performed using the CrysAlisPro program. The intensities were corrected for Lorentz and polarization effects, and numerical absorption correction based on gaussian integration over a multifaceted crystal model was applied. The structure was solved by direct methods using SHELXT,[32] which revealed the positions of all not disordered non-hydrogen atoms of the title compound. The non-hydrogen atoms were refined anisotropically. All H-atoms were placed in geometrically calculated positions and refined using a riding model where each H-atom was assigned a fixed isotropic displacement parameter with a value equal to 1.2Ueq of its parent atom (1.5Ueq for the methyl groups and water). Refinement of the structure was carried out on F^2 using full-matrix least-squares procedures, which minimized the function $\Sigma w(F_o^2 – F_c^2)^2$. The weighting scheme was based on counting statistics and included a factor to downweight the intense reflections. All calculations were performed using the SHELXL-2014/7[33] program. Further crystallographic details are compiled in Tables S2–8.

Crystallographic data for all structures have been deposited with the Cambridge Crystallographic Data Centre (CCDC) as supplementary publication numbers **4a** (2026204), **4b** (2026205), **4c** (2026206), **5** (2026207), **6** (2026208), **11** (2026209), and **12** (2026210).

Supporting Information. NMR spectra, kinetic and crystallographic data.

Acknowledgements: We acknowledge generous financial support from the European Research Council (CoG 615653) and from the Swiss National Science Foundation (200020_182663). We thank the group of Chemical Crystallography of the University of Bern for X-ray analysis of all reported structures.

References

(1) Pearson, R. G. *Chem. Rev.* **1985**, *85*, 41.

(2) Ley, M. B.; Jepsen, L. H.; Lee, Y.; Cho, Y. W.; von Colbe, M. B.; Dornheim, M.; Rokni, M.; Jensen, J. O.; Sloth, M.; Filinchuk, Y.; Jørgensen, J. E.; Besenbacher, F.; Jensen, T. R. *Mater. Today* **2014**, *17*, 122.

(3) Mohtadi, R.; Orimo, S. *Nat. Rev.* **2016**, *2*, 1.

(4) Clapham, S. E.; Hadzovic, A.; Morris, R. H. *Coord. Chem. Rev.* **2004**, *248*, 2201.

(5) Bullock, R. M. *Chem. Eur. J.* **2004**, *10*, 2366.

(6) Robertson, A.; Matsumoto, T.; Ogo, S. *Dalton Trans.* **2011**, *40*, 10304.

(7) Wang, D.; Astruc, D. *Chem. Rev.* **2015**, *115* (13), 6621.

(8) Hassam, M.; Taher, A.; Arnott, G. E.; Green, I. R.; Otterlo, W. A. L. Van. *Chem. Rev.* **2015**, *115*, 5462.

(9) Hilt, G. *ChemCatChem* **2014**, *6*, 2484.

(10) Labinger, J. A.; Bercaw, J. E. *Nature* **2002**, *417*, 507.

(11) Lyons, T. W.; Sanford, M. S. *Chem.Rev.* **2010**, *110*, 1147.

(12) Engle, K. M.; Mei, T.; Wasa, M.; Yu, J. *Acc. Chem. Res.* **2012**, *45*, 788.

(13) Choi, J.; Macarthur, A. H. R.; Brookhart, M.; Goldman, A. S. *Chem. Rev.* **2011**, *111*, 1761.

(14) Wiedner, E. S.; Chambers, M. B.; Pitman, C. L.; Bullock, R. M.; Miller, A. J. M.; Appel, A. M. *Chem. Rev.* **2016**, *116* (15), 8655.

(15) Orimo, S.-I.; Nakamori, Y.; Eliseo, J. R.; Zuttel, A.; Jensen, C. M. *Chem. Rev.* **2007**, *107*, 4111.

(16) Olivares, M.; van der Ham, C. J. M.; Mdluli, V.; Schmidtendorf, M.; Müller-Bunz, H.; Verhoeven, T. W. G. M.; Li, M.; Niemantsverdriet, J. W.; Hetterscheid, D. G. H.;

Bernhard, S.; Albrecht, M. *Eur. J. Inorg. Chem.* **2020**, *2020* (10), 801.

(17) Olivares, M.; Knörr, P.; Albrecht, M. *Dalton Trans.* **2020**, *49* (6), 1981.

(18) Gründemann, S.; Kovacevic, A.; Albrecht, M.; Faller, J. W.; Crabtree, R. H. *Chem. Commun.* **2001**, *4* (21), 2274.

(19) Gründemann, S.; Limbach, H.-H.; Buntkowsky, G.; Sabo-Etienne, S.; Chaudret, B. *J. Phys. Chem. A* **1999**, *103* (24), 4752.

(20) Gründemann, S.; Kovacevic, A.; Albrecht, M.; Faller, J. W.; Crabtree, R. H. *J. Am. Chem. Soc.* **2002**, *124* (35), 10473.

(21) Complex **6** containing –OEt substituent did not show any peculiar bond lengths or angles as observed for the analogous Cp* complex,[16] which showed an unusually large Ir–C_{trz} distance that is counterbalanced by short Ir–Cl and Ir–Cp* bonds, as well as a remarkably long C_{trz}–C_{trz} bond close to that of single bonds (1.472 Å). In complex **6**, this C_{trz}–C_{trz} distance is 1.380 Å, in line with the typically observed conjugated double bond character.

(22) For examples, see: a) Crabtree, R. H.; Mella, M. F.; Mihelcic, J. M. *Inorg. Synth.* **1990**, *28*, 56; b) Kaska ; c) Goldberg, J. M.; Goldberg, K. I.; Heinekey, D. M.; Burgess, S. A.; Lao, D. B.; Linehan, J. C. *J. Am. Chem. Soc.* **2017**, *139*, 12638.

(23) For examples, see: a) Crabtree, R. H.; Lavin, M.; Bonneviot, L. *J. Am. Chem. Soc.* **1986**, *108*, 4032; b) Heinekey, D. M.; van Roon, M. *J. Am. Chem. Soc.* **1996**, *118*, 12134; c) Li, X., Appelhans, L. N.; Faller, J. W.; Crabtree, R. H. *Organometallics* **2004**, *23*, 3378; d) Appelhans, L. N.; Zuccaccia, D.; Kovacevic, A.; Chianese, A. R.; Miecznikowski, J. R.; Macchioni, A.; Clot, E.; Eisenstein, O.; Crabtree, R. H. *J. Am. Chem. Soc.* **2005**, *127*, 16299; e) Chianese, A. R.; Kovacevic, A.; Zeglis, B. M.; Faller, J. W.; Crabtree, R. H. *Organometallics* **2004**, *23*, 2461.

(24) Lee, D.-H.; Patel, B. P.; Clot, E.; Eisenstein, O.; Crabtree, R. H. *Chem. Commun.* **1999**, 297

(25) Brereton, K. R.; Smith, N. E.; Hazari, N.; Miller, A. J. M. *Chem. Soc. Rev.* **2020**. doi:10.1039/d0cs00405g

(26) Morris, R. H. *J. Am. Chem. Soc.* **2014**, *136* (5), 1948.

(27) HNO_3 was added as a 60% aqueous solution, which perturbed the homogeneity of the reaction mixture that may account for the observed deviation.

(28) Slightly lower k_{obs} were obtained from the ^{1}H NMR data compared to the ^{31}P NMR analysis, most likely due to the limited accuracy of integration in the hydride area.

(29) Crabtree, R. H.; Felkin, H.; Morris, G. E. *J. Organomet. Chem.* **1977**, *141*, 205.

(30) CrysAlisPro (Version 1.171.34.44). Oxford Diffraction Ltd., Yarnton, Oxfordshire, UK, **2010**.

(31) Macchi, P.; Bürgi, H. B.; Chimpri, A. S.; Hauser, J.; Gál, Z. *J. Appl. Crystallogr.* **2011**, *44* (4), 763.

(32) Sheldrick, G. M. *Acta Crystallogr. A* **2015**, *71* (1), 3.

(33) Sheldrick, G. M. *Acta Crystallogr. C* **2015**, *71*, 3.

Hydride references:

IrH2L2P2]+ Crabtree, R. H.; Mella, M. F.; Mihelcic, J. M. *Inorg. Synth.* **1990**, *28*, 56; bq-IrH(H2): trans(PCP)Ir(H)2CO: Goldberg, J. M.; Goldberg, K. I.; Heinekey, D. M.; Burgess, S. A.; Lao, D. B.; Linehan, J. C. *J. Am. Chem. Soc.* **2017**, *139*, 12638.

Bbq-NH2:

; Crabtree, R. H.; Lavin, M.; Bonneviot, L. *J. Am. Chem. Soc.* **1986**, *108*, 4032; P(P)3IrH2: Heinekey, D. M.; van Roon, M. *J. Am. Chem. Soc.* **1996**, *118*, 12134. IrH2LL'P2: Li, X., Appelhans, L. N.; Faller, J. W.; Crabtree, R. H. *Organometallics* **2004**, *23*, 3378. IrH2P2(carb)(py): Appelhans, L. N.; Zuccaccia, D.; Kovacevic, A.; Chianese, A. R.; Miecznikowski, J. R.; Macchioni, A.; Clot, E.; Eisenstein, O.; Crabtree, R. H. *J. Am. Chem. Soc.* **2005**, *127*, 16299. Chianese, A. R.; Kovacevic, A.; Zeglis, B. M.; Faller, J. W.; Crabtree, R. H. *Organometallics* **2004**, *23*, 2461.

For table of contents entry only: